The Heart Surgery Forum

Heart Surg. Forum **2026**; 29(6): 51865
https://doi.org/10.31083/HSF51865

Article

An Explainable Machine Learning Model for Predicting Enteral Nutrition Feeding Intolerance in ICU Patients After Cardiopulmonary Bypass-Assisted Cardiac Surgery

Xueqing Chen[1], Shengqiang Zou[2,*], Yiting Wang[3], Jing Li[4], Ruijie Zong[4], Weiwei Chen[1], Yin Fang[1]

[1]School of Medicine, Jiangsu University, 212013 Zhenjiang, Jiangsu, China
[2]Department of Critical Care Medicine, Zhen Jiang Third Hospital Affiliated to Jiangsu University, 212013 Zhenjiang, Jiangsu, China
[3]Department of Anesthesiology, Affiliated Hospital of Jiangsu University, 212001 Zhenjiang, Jiangsu, China
[4]Department of Cardiovascular Surgery Intensive Care Unit, The First Affiliated Hospital of Anhui Medical University, 230032 Hefei, Anhui, China
*Correspondence: 1210xyz@163.com (Shengqiang Zou)

Academic Editor: Nicholas R. Teman
Submitted: 13 March 2026 Revised: 18 April 2026 Accepted: 24 April 2026 Published: 17 June 2026

Abstract

Background: Enteral nutrition (EN) feeding intolerance (ENFI) frequently occurs in intensive care unit (ICU) patients after cardiopulmonary bypass (CPB)-assisted cardiac surgery and may adversely affect postoperative recovery. However, predictive tools specifically tailored to this population remain limited. This study aimed to develop and validate an explainable machine learning model to predict ENFI in postoperative ICU patients following CPB-assisted cardiac surgery. **Methods:** This retrospective study included 519 adult patients admitted to the ICU following CPB-assisted cardiac surgery between June 2019 and December 2023. ENFI was assessed within 5 days of EN initiation according to standardized clinical criteria. Thirty-nine perioperative variables were collected. The dataset was randomly divided into a training cohort (70%) and a testing cohort (30%). Least absolute shrinkage and selection operator (LASSO) regression was applied for feature selection within the training cohort. Five machine learning algorithms, including support vector machine (SVM), random forest (RF), decision tree (DT), naïve Bayes (NB), and extreme gradient boosting (XGBoost), were developed and compared. Model performance was evaluated using area under the receiver operating characteristic curve (AUC), calibration analysis, Brier score, and decision curve analysis (DCA). Shapley Additive Explanations (SHAP) were used to enhance interpretability. **Results:** Among the 519 patients, 253 (48.7%) developed ENFI. Fourteen predictors were selected by LASSO regression. In the independent testing cohort, the RF model demonstrated the highest discriminative performance, with an AUC of 0.864 (95% confidence interval [CI]: 0.804–0.916), sensitivity of 0.747, specificity of 0.815, and a Brier score of 0.155. Calibration curves indicated good agreement between predicted and observed probabilities, and DCA demonstrated favorable net clinical benefit across a range of threshold probabilities. SHAP analysis identified vasoactive-inotropic score (VIS), serum creatinine, lactate, delayed EN, and estimated glomerular filtration rate (eGFR) as the most influential predictors. **Conclusions:** An explainable machine learning model, particularly the RF algorithm, showed good discrimination and calibration for predicting ENFI in ICU patients after CPB-assisted cardiac surgery. The identified predictors highlight the importance of hemodynamic instability and organ dysfunction in the development of ENFI and may support early risk stratification and individualized nutritional management in postoperative ICU patients. However, as this model was developed and internally validated in a single-center cohort, further external validation in independent populations is required before broader clinical application.

Keywords: enteral nutrition feeding intolerance; cardiac surgery; cardiopulmonary bypass; machine learning; random forest; intensive care unit

1. Introduction

Cardiac surgery requiring cardiopulmonary bypass (CPB) remains a cornerstone treatment for complex structural and ischemic heart diseases [1]. Although surgical techniques and perioperative management have improved substantially [2], patients requiring intensive care unit (ICU) admission after CPB continue to experience significant physiological stress [3], systemic inflammatory activation [4], and hemodynamic instability [5]. These disturbances predispose them to organ dysfunction [6], prolonged mechanical ventilation [7], infectious complications [8], and increased mortality [9]. Therefore, optimizing supportive care strategies in this vulnerable population remains a critical component of postoperative management.

Adequate nutritional support is an essential element of modern critical care [10]. Current guidelines recommend early initiation of enteral nutrition (EN) in hemodynamically stable ICU patients [11], including those undergoing cardiac surgery [12], as early EN may help maintain gut integrity and improve outcomes [13,14,15]. However, in clinical practice, enteral feeding intolerance (ENFI) frequently limits effective nutritional delivery, particularly following

CPB [16]. The mechanisms underlying ENFI in this setting are multifactorial and may include transient splanchnic hypoperfusion [17], exposure to vasoactive agents and sedatives [18], postoperative ileus [19], and systemic inflammatory responses [20]. Clinically, ENFI manifests as gastric residual accumulation, vomiting, abdominal distension, diarrhea, or failure to achieve prescribed caloric targets [21], often leading to feeding interruption and cumulative energy deficits. Importantly, ENFI has been linked to extended ICU stays, infection complications, and a higher risk of mortality, underscoring its clinical significance [22].

Given these consequences, the early recognition of individuals at an elevated risk of ENFI is clinically desirable. Previous investigations into predictors of feeding intolerance in critically ill patients have largely relied on conventional regression-based approaches [23,24]. Although informative, these methods typically assume linear relationships and include a limited number of variables [25], which may not adequately capture the complex interactions among hemodynamic instability, inflammatory activation, medication exposure, and organ dysfunction that characterize the post-CPB period [26].

In this context, machine learning techniques are increasingly used as an effective approach for risk assessment in critical care [27]. By accommodating high-dimensional data and modeling nonlinear associations, machine learning algorithms are better suited to address the multifactorial and dynamic nature of postoperative critical illness [28]. Recent studies have applied machine learning methods to predict ENFI in general ICU populations, reporting encouraging predictive performance [29,30]. However, these investigations were conducted in heterogeneous ICU cohorts, and their applicability to patients undergoing CPB remains uncertain [31]. In addition, concerns regarding the explainability of machine learning models have limited their use in clinical practice. Recently, methods within explainable artificial intelligence, including Shapley Additive Explanations (SHAP), have been introduced to enhance model interpretability [32].

Against this background, there remains a need for predictive models specifically developed for ICU patients following CPB-assisted cardiac surgery. Therefore, this study was designed to develop and validate machine learning-based models to predict ENFI in this high-risk population. Furthermore, we incorporated explainable artificial intelligence techniques to elucidate the perioperative risk pattern and enhance clinical interpretability of the model outputs.

2. Methods

2.1 Study Population

The study design and analytical workflow were illustrated in Fig. 1. This retrospective study enrolled adult patients undergoing cardiac surgery with CPB, all of whom were subsequently admitted to the ICU at the First Affiliated Hospital of Anhui Medical University between June 2019 and December 2023. After applying predefined inclusion and exclusion criteria, 519 patients were ultimately retained for analysis.

The study was approved by the Clinical Research Ethics Committee of the First Affiliated Hospital of Anhui Medical University (Approval No. PJ 2025-01-78; approved on March 20, 2025). All patient data were de-identified prior to analysis; informed consent was not required due to the retrospective study design. The inclusion criteria included: (a) Age ≥18 years; (b) Underwent cardiac surgery with CPB and were admitted to the ICU postoperatively; (c) Received EN via nasogastric or nasoenteric tube; (d) EN duration ≥24 hours; and (e) Complete clinical data available. Exclusion criteria included: (a) History of gastrointestinal disease or prior gastrointestinal surgery; (b) Initiation of EN prior to ICU admission; and (c) Incomplete clinical records.

2.2 Data Collection

To develop a clinically applicable prediction model, candidate predictors were identified through a structured literature review and expert consultation. Variables were selected according to clinical relevance and their routine availability in clinical practice. Ultimately, 39 candidate variables were included for model development.

These variables were categorized into four domains: preoperative variables, intraoperative variables, first laboratory results within 24 hours after ICU admission, and treatment-related variables prior to initiation of EN.

(1) Preoperative Variables. Sex, age, height, weight, body mass index (BMI), a history of hypertension, diabetes mellitus, hyperlipidemia, or prior cerebral infarction, New York Heart Association (NYHA) functional class, and left ventricular ejection fraction (LVEF) before surgery.

(2) Intraoperative Variables. CPB duration, aortic cross-clamp time, operative time, lactate, and surgical type (valvular surgery, great vessel surgery, combined valvular surgery and coronary artery bypass grafting, surgical repair of congenital heart disease, coronary artery bypass grafting, other cardiac procedures).

(3) First laboratory results within 24 hours after ICU admission. White and red blood cell count, platelet count, hemoglobin, hematocrit, serum albumin, serum alanine aminotransferase (ALT) and aspartate aminotransferase (AST), serum creatinine, estimated glomerular filtration rate (eGFR), activated partial thromboplastin time (APTT), D-dimer, serum potassium, and bicarbonate levels.

(4) Treatment-related variables prior to EN initiation. Delayed extubation, vasoactive-inotropic score (VIS), delayed EN, use of anti-arrhythmic agents, sedatives, opioid analgesics, antibiotic therapy (single vs. combined), Nutritional Risk Screening 2002 (NRS-2002) score, and Acute Physiology and Chronic Health Evaluation II (APACHE II) score were assessed within 24 hours following ICU admission. Delayed extubation was defined as extubation occur-

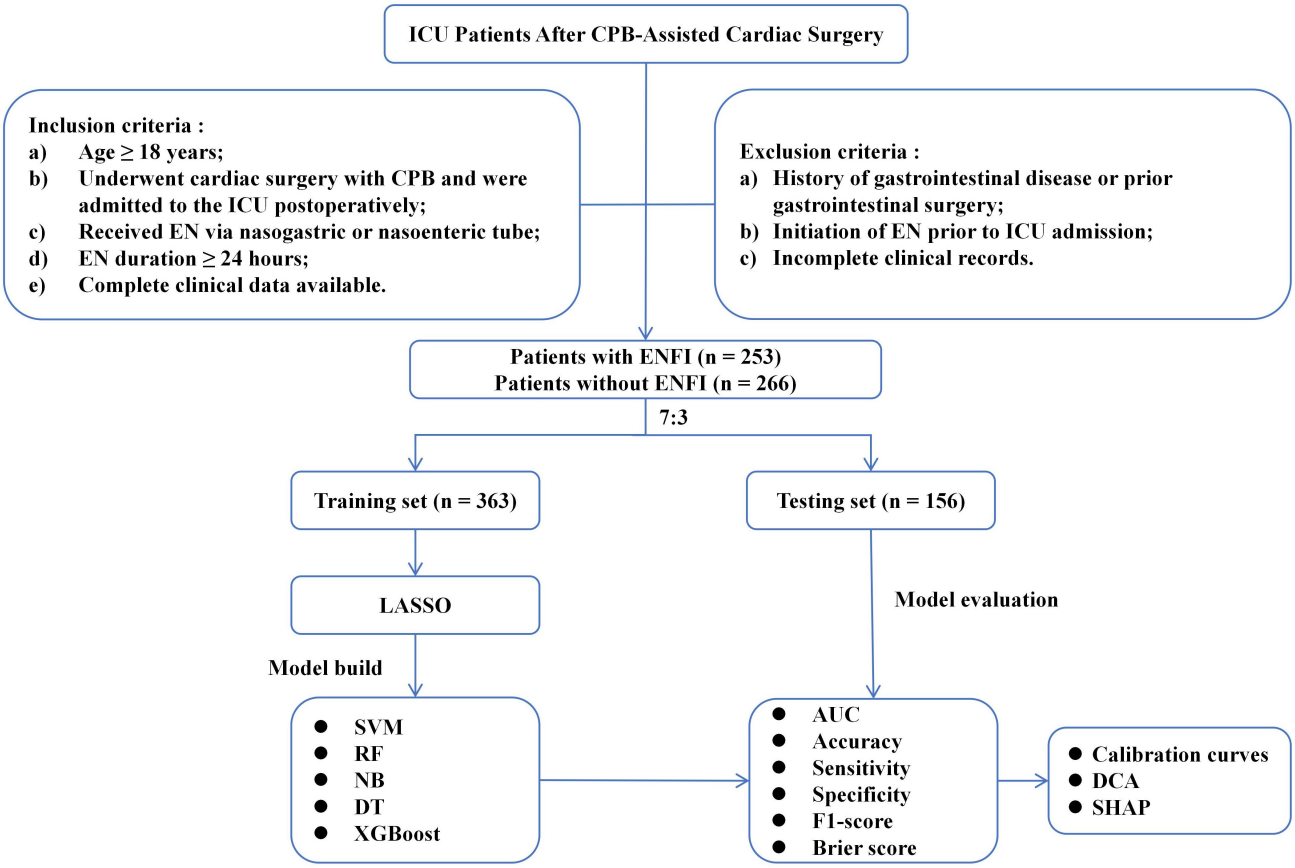

Fig. 1. Study workflow. ICU, intensive care unit; CPB, cardiopulmonary bypass; EN, enteral nutrition; ENFI, enteral nutrition feeding intolerance; LASSO, least absolute shrinkage and selection operator; SVM, support vector machine; RF, random forest; NB, naïve Bayes; DT, decision tree; XGBoost, extreme gradient boosting; AUC, the area under the receiver operating characteristic curve; DCA, decision curve analysis; SHAP, Shapley Additive Explanations.

ring later than 24 hours after ICU admission, while delayed EN referred to initiation of EN later than 48 hours after ICU admission.

Clinical data were collected from the electronic medical record and nursing documentation system of the First Affiliated Hospital of Anhui Medical University. All predictor variables were collected prior to the initiation of EN. To ensure data accuracy and reliability, two trained investigators independently collected data using a standardized data extraction form. Any discrepancies between the two datasets were reviewed and adjudicated by a third senior investigator.

2.3 Assessment of ENFI

According to the definition of feeding intolerance proposed by the Abdominal Problems Working Group within the European Society of Intensive Care Medicine [33], together with evidence from previous ICU studies, ENFI was assessed within 5 days of EN initiation among ICU patients following cardiac surgery.

ENFI was defined as the occurrence of gastrointestinal symptoms that interfered with the continuation or advancement of EN, including: (1) vomiting or reflux, defined as visible expulsion of gastric contents or regurgitation of enteral formula; (2) diarrhea, defined as three or more episodes of loose or watery stools within a 24-hour period; (3) abdominal distension requiring clinical intervention or adjustment of EN and/or (4) high gastric residual volume, which was defined as either a single measurement ≥300 mL requiring intervention or a cumulative volume ≥500 mL over 24 hours [30].

Failure to achieve target energy delivery due to planned hypocaloric feeding strategies or transient hemodynamic instability in the early postoperative period was not considered ENFI. Patients who tolerated EN without the above gastrointestinal manifestations, or who transitioned to full oral intake without symptoms, were classified as enteral feeding tolerant.

2.4 Model Development

This study was reported in line with the Transparent Reporting of a multivariable prediction model for Individual Prognosis or Diagnosis (TRIPOD) guidelines [34]. The entire dataset was randomly split into training (70%) and

testing subsets (30%). The training subset was used for feature selection, model construction, and hyperparameter optimization, whereas the testing subset served for independent evaluation of model performance. Patterns of missing data were examined to assess the underlying mechanism of missingness. The proportion of missing data for each variable is summarized in **Supplementary Table 1**. Variables with ≥20% missing values were removed from subsequent analysis. For variables with <20% missingness, missing data were handled using an iterative imputation method based on chained equations, implemented via the Python IterativeImputer. A single imputed dataset was generated. For continuous variables, bayesian ridge regression was used as the estimator, whereas for categorical variables, a random forest classifier was applied with an initial strategy of 'most frequent'. The imputation models were fitted using only the training data and subsequently applied to the testing data to avoid data leakage.

In this study, all 39 candidate predictors were simultaneously incorporated into a Least absolute shrinkage and selection operator (LASSO) regression model based on the training dataset. Before model fitting, continuous variables were scaled via z-score normalization (mean = 0, standard deviation = 1) to reduce the impact of scale differences, whereas categorical variables were transformed into dummy variables and were not normalized. LASSO regression is a regularization-based variable selection method that introduces an L1 penalty to the regression coefficients. By shrinking less informative coefficients toward zero, LASSO effectively performs both variable selection and model regularization, thereby simplifying the model and reducing the likelihood of overfitting [35]. Given that the APACHE II score is a composite clinical index derived from multiple physiological variables, it may overlap with some individual predictors included in the model. However, all candidate variables were retained during feature selection to allow the LASSO algorithm to determine their relative contributions and to account for potential complementary predictive information.

Ten-fold cross-validation was performed on the training dataset to determine the optimal regularization parameter (λ), which governs the penalty magnitude. Two λ values were obtained: λ.min, corresponding to the lowest cross-validated error, and λ.1se, representing a more parsimonious model within one standard error of the minimum. We selected λ.1se to determine the final set of predictors, as this approach balances predictive performance with clinical feasibility by retaining a limited number of relevant variables that are readily available in routine practice. Importantly, LASSO-based feature selection was performed exclusively within the training dataset after data splitting, and the independent testing dataset was not involved in any stage of feature selection, thereby avoiding potential data leakage. Variable selection stability across resampling iterations was not formally assessed, however the use of cross-validation and the λ.1se criterion was intended to improve the robustness and generalizability of the selected predictors.

Using the selected predictors, five machine learning models were developed for predicting ENFI, namely support vector machine (SVM), random forest (RF), decision tree (DT), naïve Bayes (NB), and extreme gradient boosting (XGBoost). To prevent information leakage, hyperparameter tuning was conducted exclusively within the training dataset. For each algorithm, five-fold cross-validation was performed to optimize model-specific hyperparameters and determine the optimal configuration. The optimized models were then retrained using the full training dataset and subsequently assessed on an independent testing dataset to evaluate predictive performance. Details of the hyperparameter search space and the final tuned values for each model are presented in **Supplementary Table 2** to enhance reproducibility.

Given that machine learning models are often considered "black box" approaches, SHAP was employed to improve model transparency and interpretability [36]. SHAP values were used to assess both the overall importance of predictors and their effects at the individual level on the predicted risk of ENFI. This approach enables visualization of feature contributions and directional effects, facilitating clinical interpretation and providing insights into potential underlying mechanisms associated with feeding intolerance in postoperative cardiac ICU patients. Accordingly, SHAP analysis was performed on the best-performing model.

2.5 Statistical Analysis

Baseline characteristics were analyzed in patients with and without ENFI, as well as across the training and testing datasets to evaluate the adequacy of random data splitting.

Continuous variables were evaluated for distribution using the Shapiro-Wilk test. Data with normal distribution were presented as mean ± standard deviation (SD) and were compared using either the Student's *t*-test or Welch's *t*-test based on variance homogeneity. Non-normally distributed variables were reported as median (IQR) and analyzed using the Wilcoxon rank-sum test. Categorical variables were expressed as n (%) and analyzed using the chi-square test or Fisher's exact test when appropriate.

All statistical analyses were performed using two-sided tests, with p-value < 0.05 indicating statistical significance.

2.6 Model Evaluation

The predictive performance of the machine learning models was assessed using a range of metrics, including discrimination, calibration, and clinical utility. All metrics were derived from the independent testing dataset. The final model was selected based on the highest area under the receiver operating characteristic curve (AUC) in the independent testing dataset. When multiple models

Table 1. Baseline and perioperative characteristics of patients with and without ENFI.

Variables	Patients with ENFI (n = 253)	Patients without ENFI (n = 266)	*p*-value
Male, n	179 (70.8)	164 (61.7)	0.029*
Age, (years)	60.0 (50.0–69.0)	61.0 (55.0–70.0)	0.045*
BMI, (kg/m^2)	24.8 (21.9–27.7)	24.2 (21.2–27.2)	0.103
Hypertension, n	139 (54.9)	107 (40.2)	<0.001*
NYHA functional class			0.037*
2, n	4 (1.6)	9 (3.4)	
3, n	217 (85.8)	239 (89.8)	
4, n	32 (12.6)	18 (6.8)	
LVEF, (%)	56.0 (47.0–60.0)	57.0 (51.0–60.0)	0.005*
CPB duration, (min)	186.0 (146.0–222.0)	162.0 (135.0–199.0)	<0.001*
Aortic cross-clamp time, (min)	129.0 (95.0–154.0)	110.0 (84.0–142.0)	0.002*
Operative time, (min)	400.0 (330.0–479.0)	340.0 (290.0–430.0)	<0.001*
Lactate, (mmol/L)	5.1 (2.5–8.4)	2.7 (2.1–3.7)	<0.001*
Platelet count, (10^9/L)	98.0 (71.0–143.0)	119.0 (85.0–161.0)	<0.001*
Serum albumin, (g/L)	30.1 (27.5–33.6)	30.4 (27.4–33.2)	0.748
Serum creatinine, (μmol/L)	106.5 (78.6–150.4)	77.1 (62.8–94.4)	<0.001*
eGFR, (mL/min/1.73 m^2)	65.7 ± 31.0	84.9 ± 23.7	<0.001*
D-dimer, (μg/mL)	3.0 (1.5–6.0)	1.6 (1.0–3.0)	<0.001*
Delayed extubation, n	228 (90.1)	182 (68.4)	<0.001*
VIS	22.0 (17.0–26.0)	15.0 (14.0–18.0)	<0.001*
APACHE II score	15.0 (12.0–17.0)	12.0 (10.0–14.0)	<0.001*
Delayed EN, n	162 (64.0)	47 (17.7)	<0.001*
Use of anti-arrhythmic agents, n	223 (88.1)	179 (67.3)	<0.001*
Use of sedatives, n	230 (90.9)	195 (73.3)	<0.001*
Use of opioid analgesics, n	80 (31.6)	24 (9.0)	<0.001*
Antibiotic therapy: combined, n	227 (89.7)	172 (64.7)	<0.001*

Values are presented as mean ± standard deviation (SD), median (interquartile range, IQR), or n (%), as appropriate. Continuous variables were compared using Student's *t*-test, Welch's *t*-test, or the Wilcoxon rank-sum test, as appropriate. Categorical variables were compared using the chi-square test or Fisher's exact test. *p-value < 0.05; ENFI, enteral nutrition feeding intolerance; BMI, body mass index; NYHA functional class, New York Heart Association functional class; LVEF, left ventricular ejection fraction; CPB, cardiopulmonary bypass; eGFR, estimated glomerular filtration rate; VIS, vasoactive-inotropic score; APACHE II score, Acute Physiology and Chronic Health Evaluation II score; EN, enteral nutrition.

showed comparable performance, model simplicity and interpretability were also considered.

Discrimination performance was primarily evaluated using the AUC. The receiver operating characteristic (ROC) curve was generated by plotting sensitivity against the false positive rate across different probability thresholds. Additional metrics, including accuracy, sensitivity, specificity, and F1-score, were also computed to further characterize classification performance [37]. The F1-score, representing the harmonic mean of precision and sensitivity, was used to account for potential class imbalance. The optimal cutoff value was selected based on the Youden index.

Model calibration was evaluated using both the Brier score and calibration curves. The Brier score was defined as the average squared difference between predicted probabilities and observed outcomes, with lower values reflecting better model performance. Calibration curves were generated using bootstrap resampling (500 repetitions) to minimize potential optimism bias, by comparing observed event rates with predicted probabilities across risk deciles.

Clinical utility was assessed using decision curve analysis (DCA) with 500 bootstrap iterations. DCA estimates the net clinical benefit of the model across different threshold probabilities by accounting for the trade-off between false-positive and false-negative results. Model performance was compared with two default strategies: treating all patients and treating none.

All statistical analyses, model development, and model evaluation were conducted in R (version 4.5.0, R Foundation for Statistical Computing, Vienna, Austria) and Python (version 3.13.5, Python Software Foundation, Wilmington, Delaware, USA).

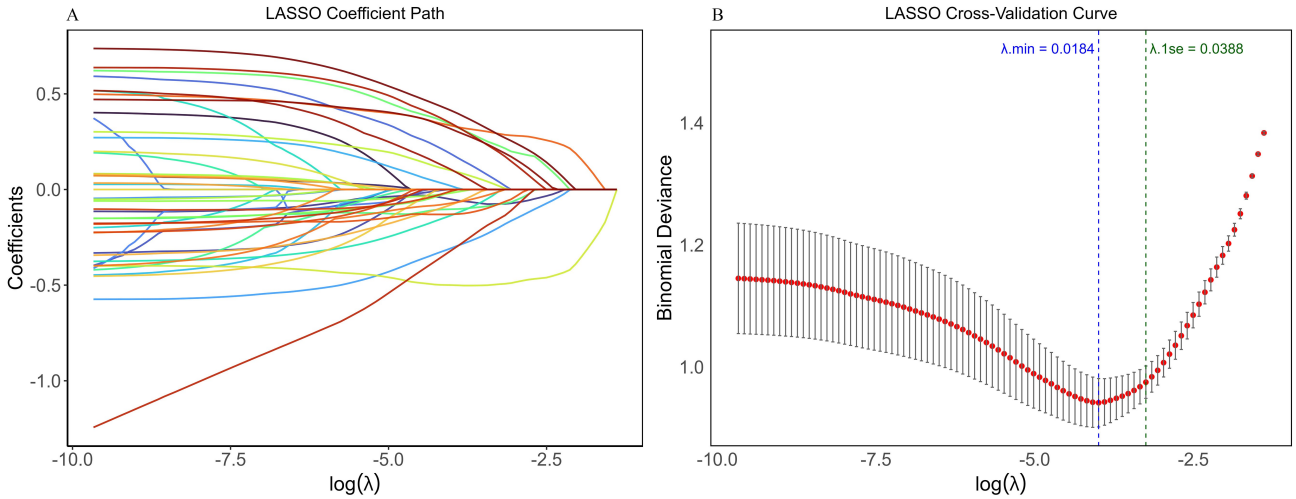

Fig. 2. Feature selection using Least absolute shrinkage and selection operator (LASSO) regression in the training cohort. (A) LASSO coefficient profiles of the 39 candidate variables plotted against log(λ), illustrating the trajectory of each variable coefficient as the penalty parameter increases. As λ increases, coefficients shrink toward zero, and variables are progressively excluded from the model. (B) Ten-fold cross-validation curve for selecting the optimal λ value. The vertical blue dashed line indicates λ.min (λ = 0.0184), corresponding to the minimum cross-validated binomial deviance, while the green dashed line represents λ.1se (λ = 0.0388), the most parsimonious model within one standard error of the minimum deviance. The λ.1se value was selected to determine the final set of predictors.

3. Results

3.1 Baseline Characteristics

A total of 519 patients were ultimately included in the analysis. Based on predefined criteria, 266 patients were categorized as enteral feeding tolerant, whereas 253 were identified as having ENFI, corresponding to an incidence of 48.7%. Baseline and perioperative characteristics of the study cohort are presented in Table 1, and 39 candidate predictors are detailed in **Supplementary Table 3**.

Patients who developed ENFI demonstrated a distinctly higher preoperative risk burden. Male sex and hypertension were more prevalent in this group ($p = 0.029$ and $p < 0.001$, respectively). Indicators of baseline disease severity differed substantially, with worse cardiac functional status as reflected by NYHA functional class ($p = 0.037$). Intraoperative features further indicated increased procedural complexity and physiological stress among patients who subsequently developed ENFI. These individuals experienced longer CPB duration and extended operative time (both $p < 0.001$), accompanied by significantly elevated lactate ($p < 0.001$). Early postoperative assessment revealed more pronounced renal dysfunction in the ENFI group. LVEF was significantly lower ($p = 0.005$), and eGFR was significantly reduced ($p < 0.001$). Before initiation of EN, patients with ENFI required greater hemodynamic support, reflected by higher VIS ($p < 0.001$), and were more likely to undergo delayed extubation ($p < 0.001$), and had higher APACHE II scores ($p < 0.001$). Delayed EN was also significantly more frequent in this group ($p < 0.001$).

3.2 Model Development

To reduce dimensionality and mitigate overfitting, LASSO regression was performed on the 39 candidate predictors in the training cohort. As illustrated in Fig. 2A, the coefficient trajectories of all 39 candidate predictors are plotted against log(λ), demonstrating how increasing penalization progressively shrinks coefficients toward zero. Variables were sequentially excluded from the model as λ increased, and only predictors with non-zero coefficients at the selected λ value were retained. Ten-fold cross-validation was performed to identify the optimal penalty parameter (Fig. 2B). Although the minimum cross-validated binomial deviance occurred at λ.min = 0.0184, a more parsimonious λ value (λ.1se = 0.0388), corresponding to one standard error above the minimum, was chosen to improve model stability.

At λ.1se, 14 predictors with non-zero coefficients were retained for subsequent model development: age, APACHE II score, lactate, serum albumin, serum creatinine, eGFR, LVEF, NYHA functional class, VIS, delayed EN, surgical type, use of anti-arrhythmic agents, use of opioid analgesics, and antibiotic therapy. These predictors were subsequently used to develop machine learning models.

3.3 Model Performance

All 519 patients were randomly divided into training and testing cohorts at a 7:3 ratio, yielding 363 patients in the training cohort and 156 in the testing cohort. Comparisons of baseline and perioperative characteristics across all can-

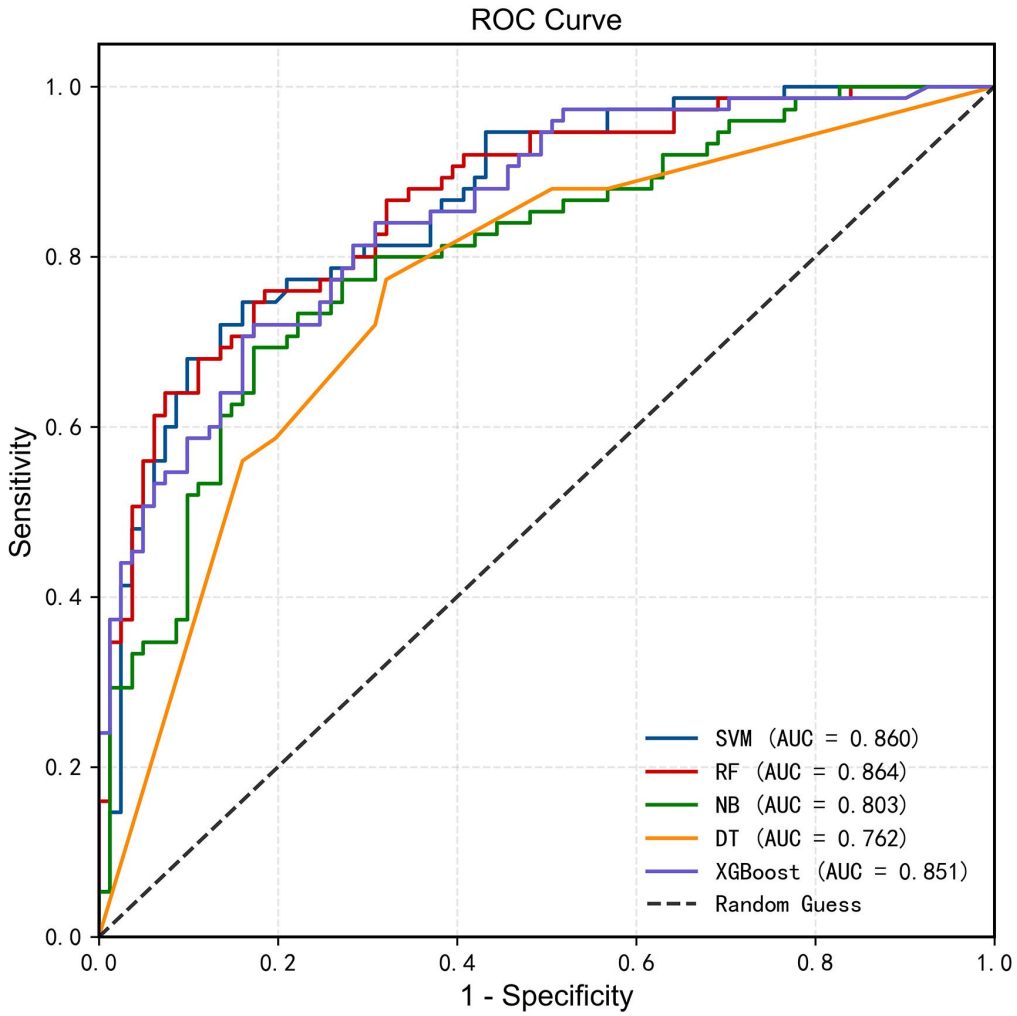

Fig. 3. Receiver operating characteristic (ROC) curves of five machine learning models in the independent testing cohort. The ROC curves illustrate the discriminative performance of the support vector machine (SVM), random forest (RF), decision tree (DT), naïve Bayes (NB), and extreme gradient boosting (XGBoost) models for predicting enteral feeding intolerance. The area under the curve (AUC) values are reported for each model, with higher AUC indicating better discrimination.

didate variables showed no significant differences between the two cohorts (**Supplementary Table 4**), supporting their comparability for subsequent model validation.

The performance of five machine learning models was assessed in the independent test cohort (Fig. 3, Table 2). Among these models, the RF classifier demonstrated the best discriminative ability, with an AUC of 0.864 (95% CI: 0.804–0.916), followed by the SVM model, which achieved an AUC of 0.860 (95% CI: 0.795–0.913). XGBoost yielded an AUC of 0.851 (95% CI: 0.791–0.903). In contrast, NB and DT demonstrated comparatively lower discriminative ability, with AUC of 0.803 (95% CI: 0.729–0.865) and 0.762 (95% CI: 0.685–0.834), respectively.

In terms of overall accuracy, SVM achieved the highest value (0.788), followed by RF (0.782), XGBoost (0.769), NB (0.756), and DT (0.705). Based on the cutoff corresponding to the highest Youden index, RF achieved the greatest sensitivity (0.747), whereas SVM exhibited slightly higher specificity (0.840 vs. 0.815). NB and XGBoost both achieved a specificity of 0.827, while DT had the lowest specificity (0.691). Regarding F1-score, SVM yielded the highest value (0.769), closely followed by RF (0.767).

Calibration performance was assessed using Brier scores (Table 2) and bootstrap-based calibration curves in the independent test cohort (Fig. 4). SVM achieved the lowest Brier score (0.153), followed closely by RF (0.155), indicating superior overall calibration compared with XGBoost (0.201), NB (0.227), and DT (0.257). Visual inspection indicated that the calibration curves of RF and SVM closely matched the observed probabilities across most risk strata and were well aligned with the ideal 45° reference line. The bootstrap-derived error bars were relatively narrow, suggesting stable probability estimation. XGBoost

Table 2. Predictive performance of five machine learning models in the independent testing cohort.

Model	AUC (95% CI)	Accuracy	Sensitivity	Specificity	F1-score	Brier score
SVM	0.860 (0.795–0.913)	0.788	0.733	0.840	0.769	0.153
RF	0.864 (0.804–0.916)	0.782	0.747	0.815	0.767	0.155
NB	0.803 (0.729–0.865)	0.756	0.680	0.827	0.729	0.227
DT	0.762 (0.685–0.834)	0.705	0.720	0.691	0.701	0.257
XGBoost	0.851 (0.791–0.903)	0.769	0.707	0.827	0.746	0.201

AUC, the area under the receiver operating characteristic curve; CI, confidence interval; SVM, support vector machine; RF, random forest; NB, naïve Bayes; DT, decision tree; XGBoost, extreme gradient boosting.

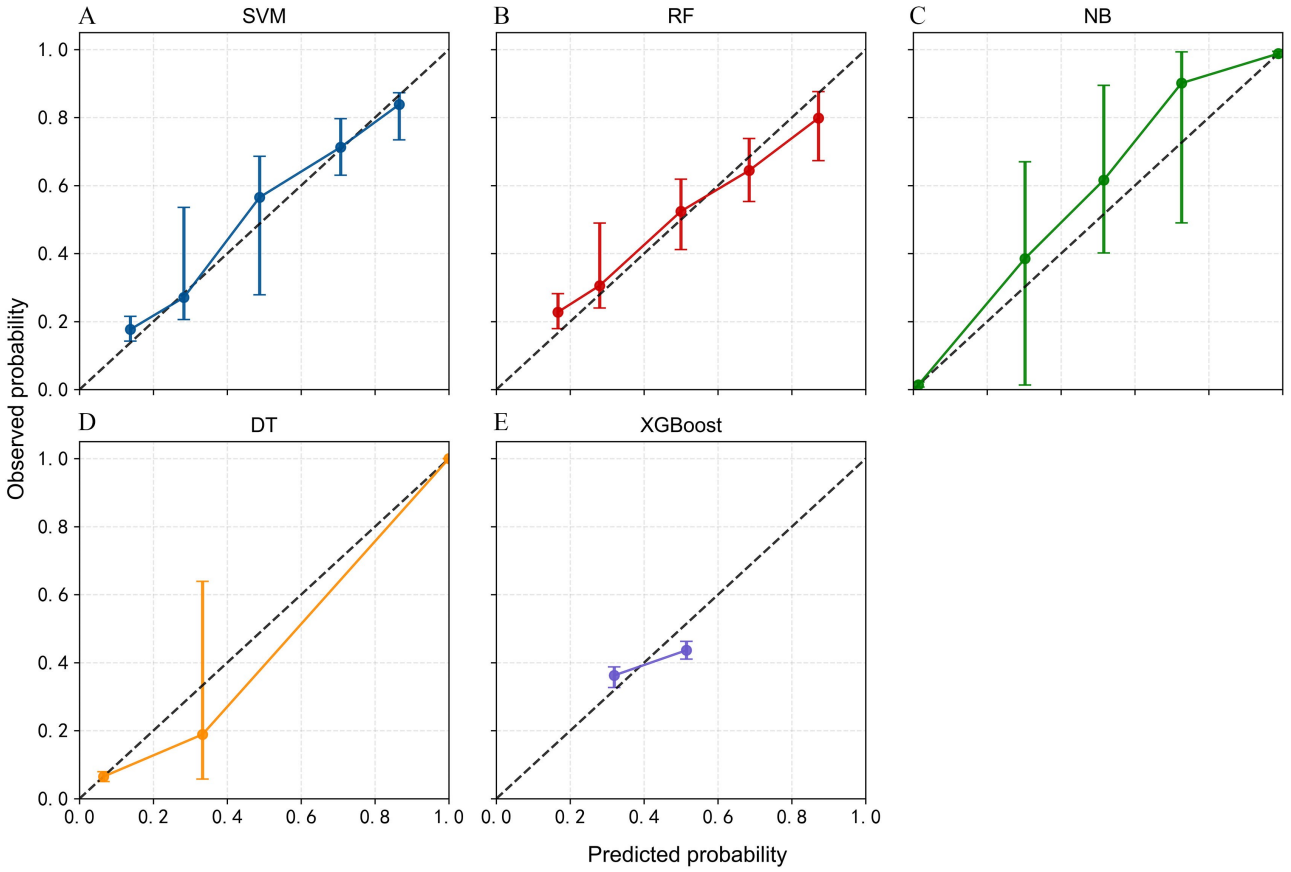

Fig. 4. Calibration curves of five machine learning models in the independent testing cohort. Calibration plots compare predicted probabilities with observed event rates of enteral feeding intolerance. The 45° diagonal line represents perfect calibration. Curves closer to the reference line indicate better agreement between predicted and observed outcomes. Bootstrap resampling (500 repetitions) was applied to reduce optimism bias. (A) Support vector machine (SVM). (B) Random forest (RF). (C) Naïve Bayes (NB). (D) Decision tree (DT). (E) Extreme gradient boosting (XGBoost).

demonstrated moderate calibration with slight deviation in the intermediate probability range. In contrast, NB and DT exhibited more pronounced departures from the reference line and wider variability, reflecting less stable probability estimation.

DCA was performed to assess the clinical usefulness of the models in the test cohort (Fig. 5). Over a wide range of clinically relevant threshold values, RF and SVM consistently provided greater net clinical benefit compared with the strategies of treating all patients or none. Although XGBoost provided positive net benefit within intermediate threshold ranges, its performance was generally inferior to that of RF and SVM. NB and DT showed limited clinical utility, with narrower threshold ranges and lower net benefit. Bootstrap resampling indicated relatively stable net benefit for RF and SVM, whereas NB and DT exhibited greater variability.

Overall, RF achieved the highest AUC in the independent test dataset, indicating superior discriminative performance among the evaluated models. Although SVM

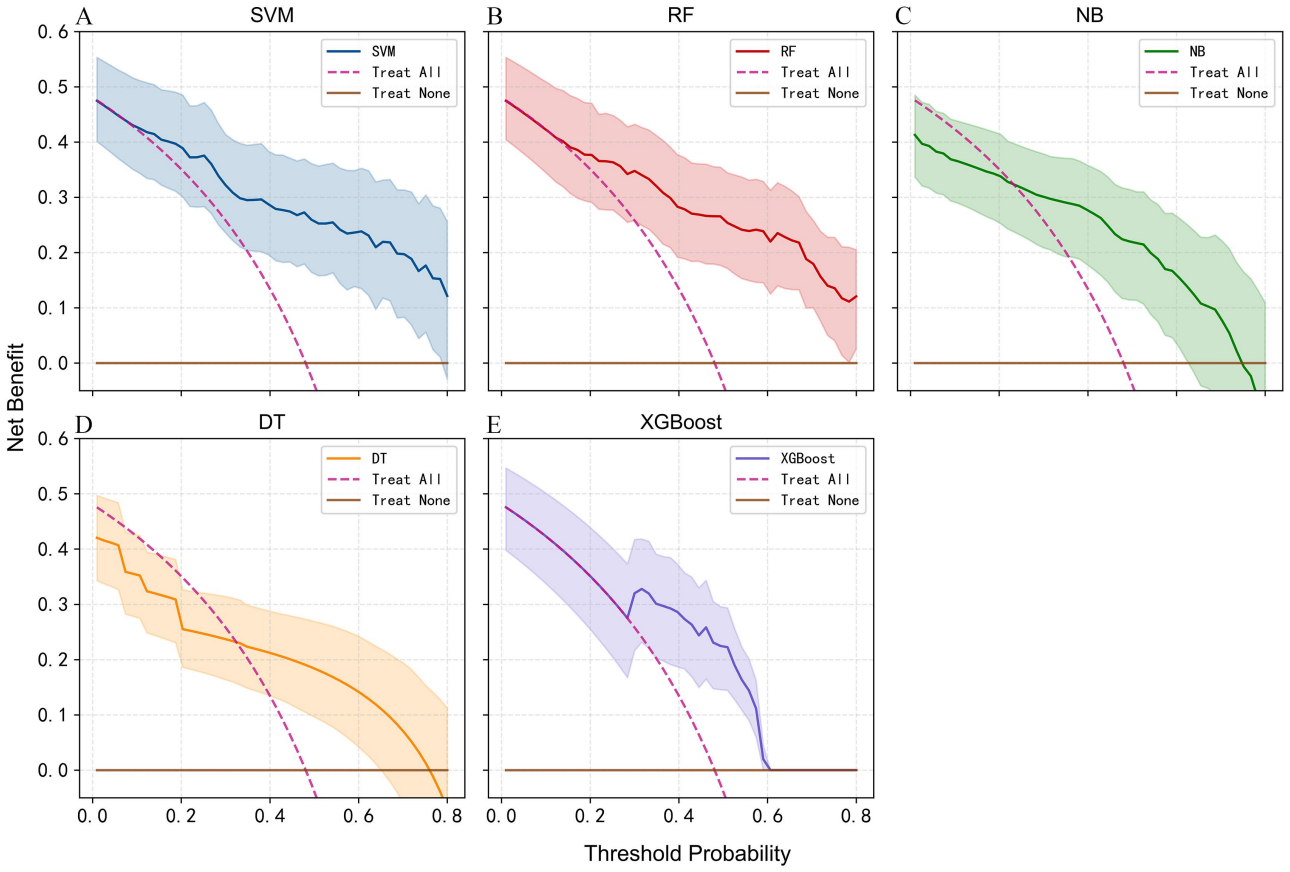

Fig. 5. Decision curve analysis (DCA) of five machine learning models in the independent testing cohort. DCA evaluates the clinical utility of each model by calculating the net benefit across a range of threshold probabilities. The pink curve represents the strategy of treating all patients, and the horizontal brown line represents treating none. Models demonstrating higher net benefit within clinically relevant threshold ranges indicate greater potential clinical usefulness. (A) Support vector machine (SVM). (B) Random forest (RF). (C) Naïve Bayes (NB). (D) Decision tree (DT). (E) Extreme gradient boosting (XGBoost).

demonstrated comparable discriminative and calibration performance, RF was selected as the final model in accordance with the prespecified model selection criteria. Specifically, when model performance was comparable, RF was preferred due to its relative simplicity and interpretability.

3.4 Model Interpretability

To improve model interpretability, SHAP analysis was applied to the RF model using the independent testing cohort. The results are presented in Fig. 6, including global feature importance (Fig. 6A), the SHAP summary distribution (Fig. 6B), and an individual-level explanation (Fig. 6C).

As shown in Fig. 6A, VIS ranked highest in terms of mean absolute SHAP value, indicating the greatest overall contribution to model output magnitude. Serum creatinine, delayed EN, lactate, and eGFR were also among the most influential predictors, demonstrating substantial average impact on predicted risk.

The SHAP summary plot (Fig. 6B) further depicts the extent and direction of feature contributions. Higher VIS levels were mainly linked to positive SHAP contributions, suggesting an elevated predicted risk of ENFI. Similarly, elevated serum creatinine, higher lactate levels, and delayed EN were mainly distributed on the positive SHAP side, suggesting that these factors contributed to higher predicted risk. In contrast, eGFR showed an inverse pattern: lower eGFR values were largely associated with positive SHAP values, whereas higher eGFR values tended to shift predictions toward lower risk. Clinical severity, as reflected by a higher APACHE II score, also demonstrated a positive association with predicted risk.

The individual force plot (Fig. 6C) provides a case-specific explanation of model prediction. For the illustrated patient, features such as antibiotic therapy, elevated VIS, and delayed EN contributed to an upward shift in predicted risk, whereas lactate and serum creatinine exerted offsetting effects. This visualization illustrates how multiple perioperative variables are combined by the model to produce an individualized risk estimate.

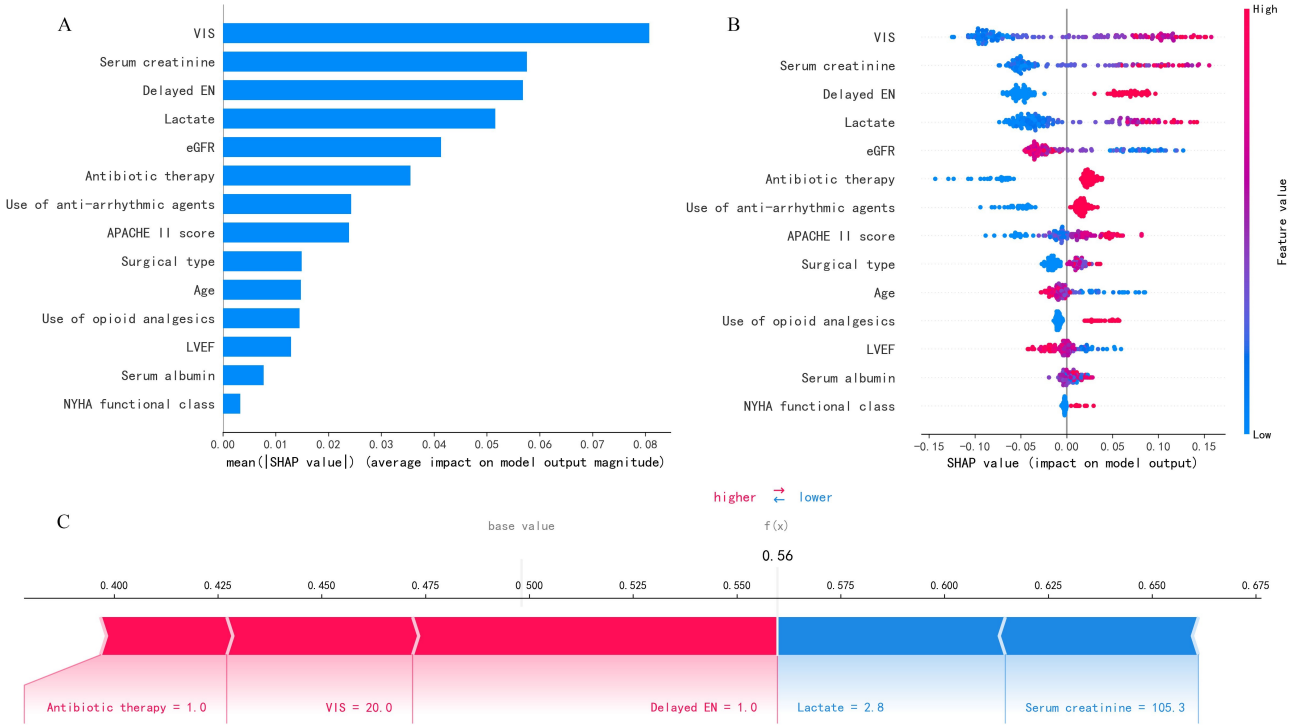

Fig. 6. SHAP-based interpretability analysis of the random forest model in the independent testing cohort. (A) Global feature importance ranked according to mean absolute SHAP values, representing the average impact of each predictor on model output magnitude. (B) SHAP summary plot showing both the magnitude and direction of feature effects. Each dot represents one patient. Positive SHAP values indicate increased predicted risk of enteral feeding intolerance, whereas negative values indicate reduced risk. Feature values are encoded by color (red = high; blue = low). (C) SHAP force plot for an individual patient. Red segments indicate features contributing to higher predicted risk, whereas blue segments indicate features with protective effects, illustrating how the prediction is derived from the base value to the final output. VIS, vasoactive-inotropic score; EN, enteral nutrition; eGFR, estimated glomerular filtration rate; APACHE II score, Acute Physiology and Chronic Health Evaluation II score; LVEF, left ventricular ejection fraction.

Overall, the SHAP analysis revealed a coherent pattern in which circulatory instability, renal dysfunction, metabolic disturbance, and delayed nutritional initiation were the principal drivers of model prediction.

4. Discussion

This study involved the development and validation of five machine learning models for predicting ENFI in ICU patients undergoing CPB-assisted cardiac surgery. Of the evaluated models, the RF model showed the best overall performance, with strong discrimination, good calibration supported by bootstrap resampling, and meaningful net clinical benefit across a wide range of clinically relevant threshold values. Importantly, SHAP-based interpretability analysis enhanced model transparency and suggested a coherent perioperative risk pattern centered on hemodynamic instability, impaired tissue perfusion, organ dysfunction, and postoperative stress response.

ENFI has been increasingly recognized as a clinically relevant complication in critically ill patients, as it is associated with prolonged mechanical ventilation, higher infection rates, and extended ICU stays [38]. In the context of cardiac surgery, ENFI may further delay recovery and complicate postoperative management. A previous study [39] in 2021 compared clinical characteristics between tolerant and intolerant patients after cardiac surgery, identifying several associated factors, however, no predictive model was constructed. In contrast, recent investigations in other critical care populations—including patients with severe acute pancreatitis and neurocritical illness—have applied logistic regression or machine learning techniques to develop predictive tools for ENFI [40,41]. While these studies highlight the feasibility of predictive modeling, their findings may not be directly generalizable to the post-CPB population [1]. To date, no study has established a dedicated predictive model for ENFI specifically in ICU patients undergoing CPB-assisted cardiac surgery.

The SHAP analysis provides important insight into the biological plausibility of the model [32]. Among all predictors, the VIS emerged as the most influential variable. Elevated VIS reflects greater dependence on vasoactive agents to maintain hemodynamic stability and serves as a surrogate marker of circulatory failure [42]. In the context of CPB, impaired myocardial performance, vasople-

gia, and systemic inflammatory response may necessitate escalating pharmacological support [43]. Increased vasoactive requirements are closely associated with compromised splanchnic blood flow. The gastrointestinal tract is particularly sensitive to hypoperfusion due to its high metabolic demand and complex microvascular regulation [44]. Reduced mesenteric perfusion can lead to mucosal ischemia, epithelial barrier dysfunction, and impaired gastrointestinal motility, all of which predispose patients to ENFI [45]. The dominant contribution of VIS in the model underscores the central role of circulatory stability in maintaining enteral feeding tolerance.

Lactate also demonstrated a strong positive association with ENFI risk. Lactate accumulation reflects an imbalance between oxygen delivery and metabolic demand and is widely recognized as an indicator of global tissue hypoperfusion [46]. In the post-CPB setting, elevated lactate may signify systemic oxygen debt and microcirculatory dysfunction [47]. From a gastrointestinal perspective, sustained or severe hyperlactatemia may correlate with splanchnic hypoxia and subsequent dysmotility [48]. The combined prominence of VIS and lactate in the SHAP ranking suggests that the model captures a "hemodynamic-metabolic axis" of risk, in which pharmacologically supported circulatory compromise and biochemical evidence of hypoperfusion jointly increase susceptibility to ENFI. These results suggest that the predictive ability of the model is not driven by any single variable, but rather by the combined contribution of variables reflecting impaired perfusion and circulatory instability. Such a pattern-based representation may explain the superior performance of the model compared with traditional approaches relying on individual risk factors. Notably, hemodynamic instability and impaired tissue perfusion—captured by variables such as VIS and lactate—have been consistently recognized as key determinants of adverse outcomes in critically ill patients [5,46], further supporting the clinical relevance and plausibility of these predictors in our model.

Renal function markers, including serum creatinine and eGFR, formed another key component of the predictive architecture. Renal dysfunction after CPB is common and reflects both ischemic injury and inflammatory-mediated damage [49]. Importantly, acute kidney injury and gastrointestinal dysfunction frequently coexist in critically ill patients, possibly due to shared mechanisms such as microvascular dysregulation, endothelial injury, and systemic inflammation [50]. Impaired renal function may also contribute to fluid overload and interstitial edema, further compromising gut wall perfusion and motility [51]. The inverse relationship between eGFR and predicted ENFI risk observed in our analysis reinforces the concept of multi-organ cross-talk, whereby renal vulnerability parallels gastrointestinal intolerance. Together, these findings suggest that the predictive value of renal-related variables in the model extends beyond kidney function itself and reflects broader systemic interactions between organ systems, reinforcing the concept that ENFI is closely linked to systemic physiological dysfunction rather than isolated gastrointestinal pathology.

Global severity indicators, particularly the APACHE II score, contributed meaningfully to model predictions, underscoring the influence of systemic physiological derangement on gastrointestinal tolerance [52]. The APACHE II score integrates multiple physiological domains and reflects the overall burden of acute illness in critically ill patients. Higher scores likely indicate intensified inflammatory activation, autonomic dysregulation, impaired organ perfusion, and metabolic stress in the early postoperative period. Such systemic instability may compromise splanchnic circulation and disrupt gastrointestinal motility and barrier integrity, thereby predisposing patients to ENFI [33]. These findings support the concept that ENFI in post-cardiac surgery ICU patients should be viewed as a manifestation of global physiological stress rather than an isolated gastrointestinal event [38]. Importantly, the simultaneous inclusion of both composite severity scores and individual physiological variables allows the model to capture risk at multiple levels, including overall disease severity and more granular physiological characteristics. This multi-level representation may enhance predictive performance and reflects a key advantage of machine learning approaches in modeling complex clinical conditions. This layered representation aligns with the complex pathophysiology of ENFI, which arises from the interaction of systemic and organ-specific processes rather than a single isolated pathway.

Perioperative management variables provided additional clinically relevant signals. Delayed EN was associated with a higher predicted risk of ENFI. Although causal inference is not possible in this retrospective analysis, delayed feeding may reflect underlying hemodynamic instability, as clinicians are often cautious in initiating enteral support in unstable patients [53]. At the same time, prolonged lack of enteral stimulation may adversely affect gut barrier function and gastrointestinal motility [54]. Previous studies [55] have suggested that early EN helps preserve mucosal integrity and support immune function. Therefore, the observed association between feeding timing and ENFI may have practical implications for individualized nutritional strategies.

From a clinical standpoint, the development of a predictive tool for ENFI in post-CPB ICU patients addresses a critical unmet need. Nutritional therapy is a cornerstone of postoperative critical care, yet intolerance often leads to feeding interruptions, and prolonged ICU stays [22]. Early identification of patients at high risk of ENFI may enable proactive strategies, including optimization of hemodynamic parameters, adjustment of vasoactive support, careful fluid management, and individualized advancement of enteral feeding. The favorable DCA observed

in our study suggests that application of the RF model may confer a meaningful net benefit compared with uniform feeding strategies. Moreover, because the included predictors are routinely available, integration into electronic clinical workflows appears feasible.

One of the key strengths of this study lies in the application of SHAP analysis to improve model interpretability. However, machine learning models are frequently criticized for limited transparency, which may hinder their adoption in clinical practice. In our analysis, the most influential predictors such as VIS, serum creatinine, and lactate are clinically plausible and consistent with mechanisms of splanchnic hypoperfusion and systemic inflammation. This concordance between model output and established physiological knowledge supports the credibility of the model and may improve clinician confidence in its application. Therefore, the RF model does not function as an isolated statistical tool, but rather reflects clinically recognizable patterns of circulatory and metabolic dysfunction associated with ENFI. Therefore, the model output is not only statistically robust but also clinically interpretable, which is essential for real-world application in critical care settings.

Taken together, our findings suggest that EN feeding intolerance in post-CPB ICU patients reflects a state of systemic physiological vulnerability characterized by circulatory instability, impaired tissue perfusion, metabolic stress, and multiorgan interaction. Rather than being merely an isolated gastrointestinal dysfunction, ENFI in this population appears to be closely linked to global hemodynamic and organ dysfunction in the early postoperative period. By integrating routinely available perioperative variables, the present model provides a clinically interpretable risk pattern that may facilitate earlier recognition of high-risk patients and support more individualized nutritional management strategies.

Limitations

Several limitations should be acknowledged. First, this study was conducted at a single center with a retrospective design, which may restrict its applicability to other cardiac surgery populations with different operative techniques, CPB management strategies, or nutritional practices. Second, although internal validation and bootstrap-based calibration were undertaken, further validation in independent multicenter cohorts is required before broader clinical application. Third, the model relied on static perioperative variables, incorporation of dynamic hemodynamic and perfusion indices may further refine prediction accuracy. Fourth, the observational design precludes causal inference regarding the identified predictors. Finally, variable selection using LASSO may be influenced by multicollinearity among predictors, and the stability of selected variables across different resampling iterations was not formally assessed. In particular, clinically related variables (e.g., serum creatinine and eGFR) may compete during penalized selection, potentially affecting the robustness of feature selection.

5. Conclusions

In this retrospective study, we developed and internally validated a machine learning-based prediction model for EN feeding intolerance in ICU patients following CPB-assisted cardiac surgery. Among the evaluated algorithms, the RF model demonstrated favorable discrimination, calibration, and potential clinical utility. The model enables early risk stratification using routinely collected perioperative data and may assist clinicians in optimizing individualized nutritional strategies in this high-risk population. However, external validation in multicenter cohorts is necessary before the model can be generalized to broader clinical settings.

Availability of Data and Materials

The datasets analyzed during the current study are available from the corresponding author upon reasonable request.

Author Contributions

XC and SZ conducted the literature review. XC, YW, and JL designed the study. XC, RZ, YF and WC performed the data analysis. XC, YF, and WC drafted the initial manuscript. All authors contributed to the critical revision of the manuscript. All authors read and approved the final manuscript. All authors have participated sufficiently in the work and agreed to be accountable for all aspects of the work.

Ethics Approval and Consent to Participate

This study was conducted in accordance with the Declaration of Helsinki. The research protocol was approved by the Clinical Research Ethics Committee of the First Affiliated Hospital of Anhui Medical University (Ethic Approval Number: PJ 2025-01-78). All patient data were de-identified prior to analysis, and the requirement for informed consent was waived due to the retrospective nature of the study.

Acknowledgment

The authors gratefully acknowledge the support provided by The First Affiliated Hospital of Anhui Medical University for this study.

Funding

This research received no external funding.

Conflicts of Interest

The authors declare no conflicts of interest.

Supplementary Material

Supplementary material associated with this article can be found, in the online version, at https://doi.org/10.31083/HSF51865.

References

[1] Ferreira LO, Vasconcelos VW, Lima JDS, Vieira Neto JR, da Costa GE, Esteves JDC, et al. Biochemical Changes in Cardiopulmonary Bypass in Cardiac Surgery: New Insights. Journal of Personalized Medicine. 2023; 13: 1506. https://doi.org/10.3390/jpm13101506

[2] Sanfilippo F, Palumbo GJ, Bignami E, Pavesi M, Ranucci M, Scolletta S, et al. Acute Respiratory Distress Syndrome in the Perioperative Period of Cardiac Surgery: Predictors, Diagnosis, Prognosis, Management Options, and Future Directions. Journal of Cardiothoracic and Vascular Anesthesia. 2022; 36: 1169–1179. https://doi.org/10.1053/j.jvca.2021.04.024

[3] Ivascu R, Torsin LI, Hostiuc L, Nitipir C, Corneci D, Dutu M. The Surgical Stress Response and Anesthesia: A Narrative Review. Journal of Clinical Medicine. 2024; 13: 3017. https://doi.org/10.3390/jcm13103017

[4] Abbasciano RG, Tomassini S, Roman MA, Rizzello A, Pathak S, Ramzi J, et al. Effects of interventions targeting the systemic inflammatory response to cardiac surgery on clinical outcomes in adults. The Cochrane Database of Systematic Reviews. 2023; 10: CD013584. https://doi.org/10.1002/14651858.CD013584.pub2

[5] Scott MJ, APSF Hemodynamic Instability Writing Group. Perioperative Patients With Hemodynamic Instability: Consensus Recommendations of the Anesthesia Patient Safety Foundation. Anesthesia and Analgesia. 2024; 138: 713–724. https://doi.org/10.1213/ANE.0000000000006789

[6] Benscoter AL, Alten JA, Atreya MR, Cooper DS, Byrnes JW, Nelson DP, et al. Biomarker-based risk model to predict persistent multiple organ dysfunctions after congenital heart surgery: a prospective observational cohort study. Critical Care. 2023; 27: 193. https://doi.org/10.1186/s13054-023-04494-7.

[7] AlRabeeah SM. A review of prolonged mechanical ventilation in pediatric cardiac surgery patients: risk factors and implications. Journal of Multidisciplinary Healthcare. 2024; 17: 6121–6130. https://doi.org/10.2147/JMDH.S494701.

[8] Massart N, Mansour A, Ross JT, Piau C, Verhoye JP, Tattevin P, et al. Mortality due to hospital-acquired infection after cardiac surgery. The Journal of Thoracic and Cardiovascular Surgery. 2022; 163: 2131–2140.e3. https://doi.org/10.1016/j.jtcvs.2020.08.094

[9] Dixon LK, Dimagli A, Di Tommaso E, Sinha S, Fudulu DP, Sandhu M, et al. Females have an increased risk of short-term mortality after cardiac surgery compared to males: Insights from a national database. Journal of Cardiac Surgery. 2022; 37: 3507–3519. https://doi.org/10.1111/jocs.16928

[10] Reignier J, Rice TW, Arabi YM, Casaer M. Nutritional Support in the ICU. BMJ (Clinical Research Ed.). 2025; 388: e077979. https://doi.org/10.1136/bmj-2023-077979

[11] Martínez-Ortega AJ, Piñar-Gutiérrez A, Serrano-Aguayo P, González-Navarro I, Remón-Ruíz PJ, Pereira-Cunill JL, et al. Perioperative Nutritional Support: A Review of Current Literature. Nutrients. 2022; 14: 1601. https://doi.org/10.3390/nu14081601

[12] Avancini L, de Abreu Silva L, da Silva VR, Duarte CK. Impact of oral or enteral nutritional support on clinical outcomes of patients subjected to cardiac surgery: A systematic review. Clinical Nutrition ESPEN. 2022; 49: 28–39. https://doi.org/10.1016/j.clnesp.2022.03.003

[13] Stoppe C, Dresen E, Wendt S, Elke G, Patel JJ, McKeever L, et al. Current practices in nutrition therapy in cardiac surgery patients: An international multicenter observational study. JPEN. Journal of Parenteral and Enteral Nutrition. 2023; 47: 604–613. https://doi.org/10.1002/jpen.2495

[14] Wang C, Sun X. Impact of early enteral nutrition on postoperative recovery in cardiac surgery patients: a cross-sectional observational study. The Heart Surgery Forum. 2024; 27: 1065–1073. https://doi.org/10.59958/hsf.7645.

[15] Zheng C, Ge Q, Luo C, Hu L, Shen Y, Xue Q. Enteral nutrition improves the prognosis and immune nutritional status of patients in the cardiothoracic surgery recovery unit: A propensity score-matched analysis. Clinical Nutrition (Edinburgh, Scotland). 2022; 41: 2699–2705. https://doi.org/10.1016/j.clnu.2022.10.012

[16] Peng Y, Chen M, Ni H, Li S, Chen L, Lin Y. Effect of timing of enteral nutrition initiation on poor prognosis in patients after cardiopulmonary bypass: A prospective observational study. Nutrition (Burbank, Los Angeles County, Calif.). 2023; 116: 112197. https://doi.org/10.1016/j.nut.2023.112197

[17] Covello LH, Castro BG, Paulillo MC, Yacoub GB, de Sousa MM, Toledo D. Enteral Nutrition in Critically Ill Patients Using Vasoactive Drugs. In Nutrition During Intensive Care. IntechOpen: London, UK. 2024. https://doi.org/10.5772/intechopen.1008215.

[18] Zhang X, Zhang J, You ZB, Zhang GF, Chen Y, Zhou XJ, et al. Effects of enteral nutrition protocols on nutritional indicators and prognosis in neurological ICU patients: a randomized controlled trial. Scientific Reports. 2025; 15: 30916. https://doi.org/10.1038/s41598-025-12650-y

[19] Issac A, Dhiraaj S, Halemani K, Thimmappa L, Mishra P, Kumar B, et al. Efficacy of Early Enteral Nutrition on Gastrointestinal Surgery Outcomes: A Systematic Review and Meta-Analysis. European Journal of Pediatric Surgery : Official Journal of Austrian Association of Pediatric Surgery ... [et Al] = Zeitschrift Fur Kinderchirurgie. 2023; 33: 454–462. https://doi.org/10.1055/s-0043-1760837

[20] Wunderle C, Stumpf F, Schuetz P. Inflammation and response to nutrition interventions. JPEN. Journal of Parenteral and Enteral Nutrition. 2024; 48: 27–36. https://doi.org/10.1002/jpen.2534

[21] Kaewdech A, Sripongpun P, Wetwittayakhlang P, Churuangsuk C. The effect of fiber supplementation on the prevention of diarrhea in hospitalized patients receiving enteral nutrition: A meta-analysis of randomized controlled trials with the GRADE assessment. Frontiers in Nutrition. 2022; 9: 1008464. https://doi.org/10.3389/fnut.2022.1008464

[22] AlElaimat M, Alshraideh JA, Darawad MW. Incidence of Enteral Nutrition-Related Diarrhea Among Critically Ill Patients in Intensive Care Units. Gastroenterology Nursing : the Official Journal of the Society of Gastroenterology Nurses and Associates. 2024; 47: 242–249. https://doi.org/10.1097/SGA.0000000000000808

[23] Lu XM, Jia DS, Wang R, Yang Q, Jin SS, Chen L. Development of a prediction model for enteral feeding intolerance in intensive care unit patients: A prospective cohort study. World Journal of Gastrointestinal Surgery. 2022; 14: 1363–1374. https://doi.org/10.4240/wjgs.v14.i12.1363

[24] Chen H, Han J, Li J, Xiong J, Wang D, Han M, et al. Risk prediction models for feeding intolerance in patients with enteral nutrition: a systematic review and meta-analysis. Frontiers in Nutrition. 2025; 11: 1522911. https://doi.org/10.3389/fnut.2024.1522911

[25] Chen Z, Hao Q, Sun R, Zhang Y, Fu H, Liu S, et al. Predictive value of the geriatric nutrition risk index for postoperative delirium in elderly patients undergoing cardiac surgery. CNS Neuroscience & Therapeutics. 2024; 30: e14343. https://doi.org/10.1111/cns.14343

[26] Zhou W, Wang H, Li C, Ma QM, Gu YH, Sheng SY, et al. Alterations in novel inflammatory biomarkers during perioperative cardiovascular surgeries involving cardiopulmonary bypass: a retrospective propensity score matching study. Frontiers in Cardiovascular Medicine. 2024; 11: 1433011. https://doi.org/10.3389/fcvm.2024.1433011
[27] Hong N, Liu C, Gao J, Han L, Chang F, Gong M, et al. State of the Art of Machine Learning-Enabled Clinical Decision Support in Intensive Care Units: Literature Review. JMIR Medical Informatics. 2022; 10: e28781. https://doi.org/10.2196/28781
[28] Chiang DH, Jiang Z, Tian C, Wang CY. Development and validation of a dynamic early warning system with time-varying machine learning models for predicting hemodynamic instability in critical care: a multicohort study. Critical Care (London, England). 2025; 29: 318. https://doi.org/10.1186/s13054-025-05553-x
[29] Liao X, Li C, Liu Q, Xia W, Liu Z, Zhu J, et al. Machine learning-based predictive model for enteral nutrition-associated diarrhea in ICU patients and its nursing applications. Frontiers in Nutrition. 2025; 12: 1584717. https://doi.org/10.3389/fnut.2025.1584717
[30] Wang G, Lu C, Solomon OM, Gu Y, Ling Y, Xu F, et al. Construction and evaluation of a machine learning-based predictive model for enteral nutrition feeding intolerance risk in ICU patients. Frontiers in Nutrition. 2025; 12: 1600319. https://doi.org/10.3389/fnut.2025.1600319
[31] Lesouhaitier M, Belicard F, Tadié JM. Cardiopulmonary bypass and VA-ECMO induced immune dysfunction: common features and differences, a narrative review. Critical Care (London, England). 2024; 28: 300. https://doi.org/10.1186/s13054-024-05058-z
[32] Prendin F, Pavan J, Cappon G, Del Favero S, Sparacino G, Facchinetti A. The importance of interpreting machine learning models for blood glucose prediction in diabetes: an analysis using SHAP. Scientific Reports. 2023; 13: 16865. https://doi.org/10.1038/s41598-023-44155-x
[33] Reintam Blaser A, Malbrain ML, Starkopf J, Fruhwald S, Jakob SM, De Waele J, et al. Gastrointestinal function in intensive care patients: terminology, definitions and management. Recommendations of the ESICM Working Group on Abdominal Problems. Intensive Care Medicine. 2012; 38(3):384–394. https://doi.org/10.1007/s00134-011-2459-y
[34] Collins GS, Reitsma JB, Altman DG, Moons KG. Transparent reporting of a multivariable prediction model for individual prognosis or diagnosis (TRIPOD): the TRIPOD statement. BMJ. 2015; 350: g7594. https://doi.org/10.1136/bmj.g7594
[35] Shaon MS, Karim T, Shakil MS, Hasan MZ. A comparative study of machine learning models with LASSO and SHAP feature selection for breast cancer prediction. Healthcare Analytics. 2024; 6: 100353. https://doi.org/10.1016/j.health.2024.100353.
[36] Ji Y, Shang H, Yi J, Zang W, Cao W. Machine learning-based models to predict type 2 diabetes combined with coronary heart disease and feature analysis-based on interpretable SHAP. Acta Diabetologica. 2025; 62: 1631–1646. https://doi.org/10.1007/s00592-025-02496-1
[37] Gan TM, Wang SR, Mo GL, Li SH, Lu YQ, Li JY. Machine learning prediction and SHAP interpretability analysis of heart failure risk in patients with hyperuricemia. Frontiers in Cardiovascular Medicine. 2025; 12: 1689607. https://doi.org/10.3389/fcvm.2025.1689607
[38] Xu J, Shi W, Xie L, Xu J, Bian L. Feeding Intolerance in Critically Ill Patients with Enteral Nutrition: A Meta-Analysis and Systematic Review. Journal of Critical Care Medicine (Universitatea De Medicina Si Farmacie Din Targu-Mures). 2024; 10: 7–15. https://doi.org/10.2478/jccm-2024-0007
[39] Liu WJ, Zhong J, Luo JC, Zheng JL, Ma JF, Ju MJ, et al. Early Enteral Nutrition Tolerance in Patients With Cardiogenic Shock Requiring Mechanical Circulatory Support. Frontiers in Medicine. 2021; 8: 765424. https://doi.org/10.3389/fmed.2021.765424
[40] Xiao W, Zeng Y, Ai L, Wang G, Fu Y. Clinical Predictors and Prevalence of Enteral Nutrition Intolerance in Acute Pancreatitis: An Updated Systematic Review and Meta-Analysis. Nutrients. 2025; 17: 910. https://doi.org/10.3390/nu17050910
[41] Yuan R, Liu L, Mi J, Li X, Yang F, Mao S. Development and validation of a risk prediction model for feeding intolerance in neurocritical patients with enteral nutrition. Frontiers in Nutrition. 2024; 11: 1481279. https://doi.org/10.3389/fnut.2024.1481279
[42] Abdallah S, Villiers T, Piccardo A, Chauvet R, Marsaud JP, Pihan F, et al. Postoperative hemodynamic stability of patients treated with the sacubritil-valsartan combination in cardiac surgery. Anaesthesia, Critical Care & Pain Medicine. 2025; 45: 101711. https://doi.org/10.1016/j.accpm.2025.101711
[43] Kontar L, Beaubien-Souligny W, Couture EJ, Jacquet-Lagrèze M, Lamarche Y, Levesque S, et al. Prolonged cardiovascular pharmacological support and fluid management after cardiac surgery. PloS One. 2023; 18: e0285526. https://doi.org/10.1371/journal.pone.0285526
[44] Davies S, Jian Z, Hatib F, Gomes A, Mythen M. DETECTION OF HYPOVOLEMIA BY THE HYPOTENSION PREDICTION INDEX IS ASSOCIATED WITH GASTROINTESTINAL MICROCIRCULATION DYSFUNCTION IN A PORCINE MODEL OF HEMORRHAGE. Shock (Augusta, Ga.). 2025; 64: 91–96. https://doi.org/10.1097/SHK.0000000000002578
[45] Garcia-Alonso I, Velasco-Oraa X, Cearra I, Iturrizaga Correcher S, Mar Medina C, Alonso-Varona A, et al. Prophylactic Treatment of Intestinal Ischemia-Reperfusion Injury Reduces Mucosal Damage and Improves Intestinal Absorption. Journal of Inflammation Research. 2023; 16: 4141–4152. https://doi.org/10.2147/JIR.S426396
[46] Kattan E, Hernández G. The role of peripheral perfusion markers and lactate in septic shock resuscitation. Journal of Intensive Medicine. 2022; 2: 17–21. https://doi.org/10.1016/j.jointm.2021.11.002
[47] Kant S, Banerjee D, Sabe SA, Sellke F, Feng J. Microvascular dysfunction following cardiopulmonary bypass plays a central role in postoperative organ dysfunction. Frontiers in Medicine. 2023; 10: 1110532. https://doi.org/10.3389/fmed.2023.1110532
[48] Kang MK, Oh SY, Lee H, Ryu HG. Pre and postoperative lactate levels and lactate clearance in predicting in-hospital mortality after surgery for gastrointestinal perforation. BMC Surgery. 2022; 22: 93. https://doi.org/10.1186/s12893-022-01479-1
[49] Milne B, Gilbey T, De Somer F, Kunst G. Adverse renal effects associated with cardiopulmonary bypass. Perfusion. 2024; 39: 452–468. https://doi.org/10.1177/02676591231157055
[50] Fiaccadori E, Maggiore U, Clima B, Melfa L, Rotelli C, Borghetti A. Incidence, risk factors, and prognosis of gastrointestinal hemorrhage complicating acute renal failure. Kidney International. 2001; 59: 1510–1519. https://doi.org/10.1046/j.1523-1755.2001.0590041510.x
[51] Meijers B, Farré R, Dejongh S, Vicario M, Evenepoel P. Intestinal Barrier Function in Chronic Kidney Disease. Toxins. 2018; 10: 298. https://doi.org/10.3390/toxins10070298
[52] Hatton GB, Madla CM, Rabbie SC, Basit AW. Gut reaction: impact of systemic diseases on gastrointestinal physiology and drug absorption. Drug Discovery Today. 2019; 24: 417–427. https://doi.org/10.1016/j.drudis.2018.11.009
[53] Yang S, Wu X, Yu W, Li J. Early enteral nutrition in critically ill patients with hemodynamic instability: an evidence-based review and practical advice. Nutrition in Clinical Practice : Official Publication of the American Society for Parenteral

and Enteral Nutrition. 2014; 29: 90–96. https://doi.org/10.1177/0884533613516167

[54] Schörghuber M, Fruhwald S. Effects of enteral nutrition on gastrointestinal function in patients who are critically ill. The Lancet. Gastroenterology & Hepatology. 2018; 3: 281–287. https://doi.org/10.1016/S2468-1253(18)30036-0

[55] Quiroz-Olguín G, Gutiérrez-Salmeán G, Posadas-Calleja JG, Padilla-Rubio MF, Serralde-Zúñiga AE. The effect of enteral stimulation on the immune response of the intestinal mucosa and its application in nutritional support. European Journal of Clinical Nutrition. 2021; 75: 1533–1539. https://doi.org/10.1038/s41430-021-00877-7